

Supercapacitor technologies to improve the power quality in dc microgrids

Bachelor thesis EE

F.R. Lacina, ir. M.B. Appelman*, I. Sulaeman, MSc*, dr. ir. D.J.G. Moonen**

University of Twente

*Daily supervisor, **Assistant Professor

Abstract—Microgrids are a promising option to achieve the energy access goal given in the united nations sustainable development goal 7 and to use more renewable energy resources. However, especially in microgrids, power quality (PQ) is still important to consider. In this research the key question is how the implementation of energy storage devices (e.g. supercapacitors (SC) and Li-ion batteries) can improve the PQ issue of voltage and current fluctuation in a microgrid, focussing on the electrical characteristics that influence the transient response to inrush current events. This is investigated by performing simulations and experiments on a 12 V dc system with transmission line model and programmable load, where such an inrush current event is simulated with an instantaneous current draw of 5 A.

SCs and Li-ion batteries have different electrical characteristics that influence the series resistance and series inductance of both. Taking this into account, simulation models have been made and simulations and measurements have been performed with both devices installed individually on both sides of the transmission line. Next to that, the series resistance and series inductance of the battery are increased to investigate the influence of both on the transient response.

The simulations and measurements showed that the response is best when the storage device is located on the load side. Furthermore, the SC gives a better response than the battery. Another finding from the simulation is, that an increased series resistance and inductance lead to a lower and slower current output, respectively.

Index Terms—Power quality, inrush current, supercapacitor, microgrid.

I. INTRODUCTION

AS of 2021, there are still 675 million people that do not have access to electricity [1]. In [2], the United Nations formulated the goal that, by 2030, everyone should have access to energy. Microgrids are a promising options to achieve this goal.

Next to that, the number of renewable energy sources has been increasing a lot over the past years. The conventional ac distribution grid is therefore not considered to be the optimal solution anymore and thus research has been done towards alternative grid structures. Also for this, dc microgrids are a promising concept for a better integration of renewable energy sources, among other things because of the increased efficiency due to less transforming stages (i.e. dc-ac-dc is not necessary, dc-dc is enough) [3].

However, especially in dc microgrids, power quality (PQ) is a huge concern because of the relatively high amount of nonlinear loads with respect to the grid size, compared to conventional distribution grids [3].

In this paper the key question is how the implementation of energy storage systems (ESS), like batteries and supercapacitors (SC), into dc microgrids improves the response to inrush current events and thus the PQ of the microgrid. The main focus lies on the differences in electrical characteristics and which option gives the best response. Based on this, the parameter defining the response is determined. Next to that, the optimal location in the microgrid setup will be investigated. This will be done using a simplified model of a 12 V dc system with a pi-section transmission line model and a programmable load.

The structure of the paper is as follows. First, the theoretical background and previous research is presented in section II. After that, the measurement setup that is used during the simulation and the experiment is explained in section III. Following that, the methods, results and discussions of the simulation and the experiment are elaborated in sections IV and V, respectively. Finally, in section VII the main conclusions are drawn and recommendations are given.

II. THEORETICAL BACKGROUND

The main goal of this research is to improve the response to high inrush current events in dc microgrids. To get a better understanding of what that exactly means, the meaning of PQ in general is explained. Since we are talking about a microgrid, it is also important to know the differences to the conventional distribution grid and how it behaves differently with respect to PQ. Finally in this section, the important aspects of modelling SCs and batteries are given.

A. PQ in general

The IEC 61000-4-30 standard describes how the PQ should be measured. In this standard, phenomena like frequency, voltage level, voltage sag or swell, interruptions as well as voltage- and current harmonics are included [4], [5].

Problems with the PQ are largely concerning because they can damage (sensitive) equipment, increase power and transmission losses, and also trigger faults in protection devices. This is only a small insight in possible problems and gives an overview of the severe impact that issues with the PQ can have [3].

B. Microgrid versus conventional grid

According to a definition from the IEC (IEV ref 617-04-22), a microgrid is a "group of interconnected loads and distributed energy resources with defined electrical boundaries forming a local electric power system at distribution voltage levels, that acts as a single controllable entity and is able to operate in either grid-connected or island mode" [6].

This means that microgrids are conceptually very different to conventional distribution grids, because the latter have large centralized power plants instead of distributed energy resources [7].

C. PQ issues in dc microgrids

The main PQ issues to consider in dc microgrids with respect to the voltage are because of inrush currents and circular currents within converters. These issues create voltage sag or swell events as well as interruptions when the issue is during a short time. When these issues hold on longer, voltage fluctuations and under-/ over-voltage events are created [8].

Voltage sag is one of the more severe PQ issues. If the voltage in the microgrid drops too low and stays there for too long, sources need to disconnect from the grid according to certain grid codes (GCs) [3].

The type of PQ issue that this research deals with is the problem of transient events that are created by high inrush currents of nonlinear loads. When such an event abruptly occurs it could happen that the grid is not able to supply the energy fast enough, especially when the supply has a comparatively large impedance. As a result the voltage drops and causes problems to (sensitive) devices.

D. Modelling of SCs and batteries

Compared to conventional capacitors, SCs have much larger electrodes and a thinner dielectric layer. Because of this, SCs have much larger capacitances and can be considered to be the component to fill the gap between conventional capacitors and batteries [9].

At the moment three main SC types are available on the market: the electric double layer capacitor (EDLC), the hybrid capacitor and the pseudocapacitor. One of the main disadvantages of SCs is the low voltage rating of only a few volts per cell. To still reach bus voltages of a few hundred volts, SCs are connected in series configurations. This has the effect that the total voltage across the module will spread evenly over the cells [9].

The maximum specific power (W/kg) is highest for the EDLC with 10,000 W/kg, and it decreases to 5000 W/kg and 4000 W/kg for the hybrid- and pseudocapacitor, respectively. However, the specific energy (W h/kg) increases from the EDLC (1 to 20 W h/kg) to 7 to 12 W h/kg and 20 to 60 W h/kg for the hybrid- and pseudocapacitor, respectively. This is because the electrochemical structure changes from a capacitor like structure for the EDLC to a more battery like structure for the pseudocapacitor [9]. Li-ion (here the NCA, $LiNi_{0.8}Co_{0.15}Al_{0.05}O_2$, is meant) and Lead-Acid batteries

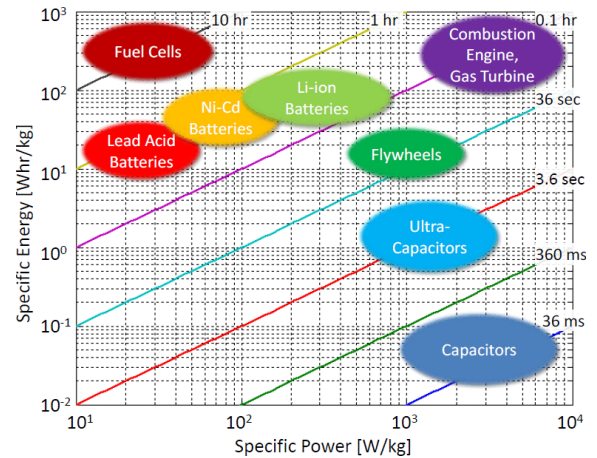


Fig. 1: Ragone plot showing the specific power (x-axis) and specific energy (y-axis) for a variety of storage devices [11]

have a specific power of 800 W/kg and 250 W/kg respectively, and a specific energy of around 150 to 180 W h/kg and 35 to 40 W h/kg respectively [10].

These values also can be seen in Fig. 1. Although this figure is a little outdated, the key message that Li-ion batteries have a higher specific energy than SCs and SCs have a higher specific power than Li-ion batteries is still valid and very clear. Comparing the Li-ion batteries with the SCs, they have up to a factor 180 higher specific energy in case of an EDLC, but also a factor 12.5 less specific power. The application will determine which of the two is more important when it comes to choosing a specific storage device.

The difference in chemical structure of all of the above mentioned components has the effect that the equivalent series resistance (ESR) and the equivalent series inductance (ESL) of all components are different.

III. MEASUREMENT SETUP

The setup that was used for this research can be seen in Fig. 2. It contains a dc power supply with a comparably large series impedance, a long cable (model), a programmable load as well as several voltage and current sensors. The RL component in the long cable model is only included on the positive terminal because later in the measurements the ground of the probes will be connected together.

The last and most important component included in the setup is the storage device. The key interest of this research is to find out what influence this storage device has on the response to the inrush current event. This storage component will be located on two different positions in the setup. These positions are referred to as load side (LS) and grid side (GS). This is indicated in the circuit diagram.

The type of storage components that are investigated are SCs and Li-ion batteries in both the simulation and the experiment. Additionally, in the simulation the impedance of the model will be varied to see the difference in the response.

This setup can be used to create an inrush current event with the programmable load and measure the response of the grid to this event. All labels (e.g. V_{grid}) included in the figure are used throughout the paper.

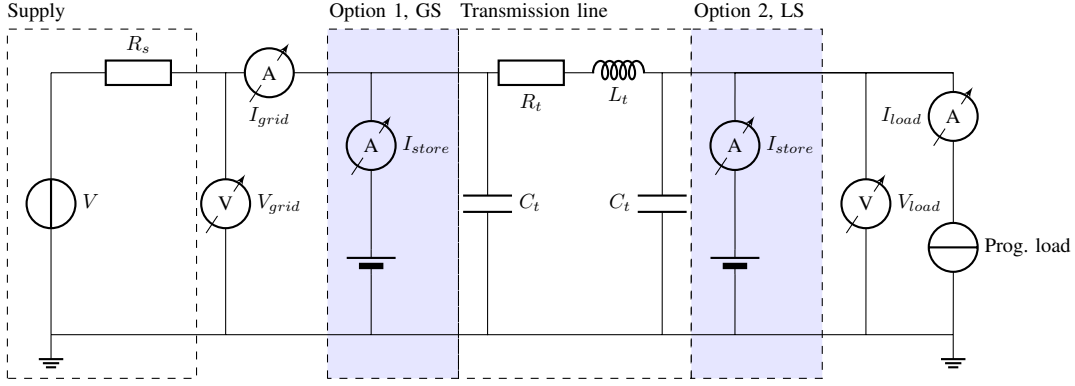


Fig. 2: Circuit diagram of the setup used in the simulation and measurement process. It includes a dc supply, a pi section lumped cable transmission line, a programmable load and a storage component that is placed on two different locations, see option 1 and 2 (but never both locations at the same time), as well as several voltage and current probes

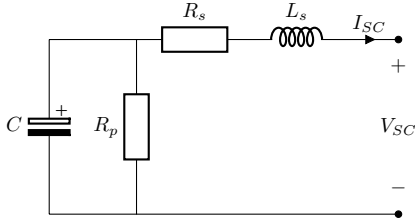


Fig. 3: SC model used in the simulation. Containing a parallel resistance R_p in parallel, as well as a series resistance R_s and inductance L_s connected to the common node of C and R_p respectively

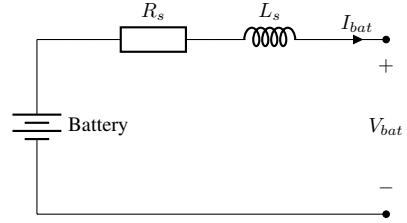


Fig. 4: Battery model used in the simulation containing the battery as well as a series resistance R_s and series inductance L_s

IV. SIMULATION STUDY

The simulation was performed using Matlab Simulink. For this the Simscape toolbox is available which offers a wide variety of ready-to-use components. As an alternative, LTspice was also considered. However, LTspice's implementation with respect to Matlab is deemed inferior to Simulink, which would increase the complexity and time needed to get a working simulation.

A. Supercapacitor model

From this point onwards, when using the term SC, the EDLC is meant. There were several attempts for a SC model, which included the two different SC models already included in the Simscape toolbox of Simulink. Together with all the other components the computation time was very long, though. Another disadvantage of using ready-to-use models is the limitation in tweaking certain values of the model. In this research the series impedance is of large interest, so for the final model the choice was made to build the model using standard RLC components. This has the advantage that the model can be as complex as needed and depending on that also has a fast simulation time. The final model can be seen in Fig. 3.

B. Battery model

In the 'Specialized Power Systems' domain, a battery model is available and ready to use. In this model the type of battery

(e.g. Li-ion, Pb-Acid, Ni-Cd and NiMH) can be chosen from a drop-down menu. Also temperature effects, ageing effects and discharge characteristics as well as the rated capacity, nominal voltage, initial state of charge (SoC) and the response time can be chosen.

For this simulation it was chosen to ignore the temperature and ageing effects to reduce simulation complexity. The SoC is simulated with 80% and 10% and the nominal voltage to 13.7 V to make it compliant with the measurements described in section V.

Finally, to be able to vary the series impedance of the battery as well, a series RL branch is included on the positive terminal of the battery as can be seen in Fig. 4.

C. Grid supply and transmission line model

The power supply modelled in the simulation is a dc source with a relatively high resistance (0.05Ω) to mimic a weak grid, i.e. the supply should be more prone to changes in the microgrid. Next to that, an almost ideal diode is included to prevent current being fed back to the supply since this is most often not possible in the real-life situation that is replicated, when e.g. a diesel engine is used as grid supply.

The pi-section transmission line model as well as the grid supply can be seen in Fig. 2. The parameters of the pi-section transmission line model are obtained from the cable used in the experiment using an LCR bridge and can be seen in Table I.

TABLE I: Component values of the pi-section transmission line, the parameters were measured from the cable using an LCR bridge

Component	Value
R_t	17.92 m Ω
L_t	1.3437 μ H
C_t	4.9 mF

D. Simulation process

The primary simulation was performed in 4 steps, each changing one component.

- 1) SC located at the LS
- 2) SC located at the GS
- 3) Battery located at the LS
- 4) Battery located at the GS

After these simulations were performed, the resistance and inductance of the battery were varied independently from each other to see the influence of both. This was done by increasing the resistance from 0.1 Ω to 1 Ω and after that increasing the inductance from 0.5 μ H to 50 μ H.

E. Results

The parameters used in the simulation with SCs can be obtained from Table II, the parameters used in the simulations with batteries can be obtained from Table III.

TABLE II: Model parameters used in the simulations with SC, parameters obtained from [12]

Component	Value
C	350 F
R_p	10 M Ω
R_s	3.5 $\mu\Omega$
L_s	5 nH

TABLE III: Model parameters used in the simulations with battery

Component	Value in Fig. 6, 7 and 8	Value in Fig. 9a	Value in Fig. 9b
R_s	0.1 Ω	0.1 Ω	1 Ω
L_s	0.5 μ H	50 μ H	0.5 μ H

In Fig. 5, the response to a 5 A inrush current event with SCs installed at the load- and grid side can be seen.

As can be seen from the figure, the SC current (I_{store}) drops much faster when the SC is installed at the GS (solid lines). This behaviour can also be seen for the voltage at the LS, which drops faster when the SC is installed at the GS. The grid current is in both cases the counterpart of the SC current.

Fig. 6 shows the response to the 5 A inrush current event with a Li-ion battery having 80% State of Charge (SoC), installed at the load side(dashed lines) and grid side (solid lines). The same simulations have been performed with 10% SoC. These results can be seen in Fig. 7.

A difference in response between the GS and LS installation can be denoted by the different voltage levels between the GS and the LS. In steady state, the voltage level is 13.9 V at the LS and 14 V at the GS. However, when the battery is installed

at the LS, the voltage level is the same at both sides. When comparing the different SoC levels of 80% and 10%, it can be seen that the grid supply (I_{grid}) only has become active once the battery drains and its current output drops. Besides the difference in GS and LS voltage for the GS installation, there is no difference in e.g. the time when the battery current starts to decrease. Only the slope is higher (i.e. faster discharge) when the battery is installed at the GS.

In Fig. 9a and 9b the resistance and inductance were changed to 1 Ω and 50 μ H, respectively. Since only the very short time at the impact of the inrush current event is important here, a version with adjusted x axes of Fig. 7 is given in Fig. 8.

F. Discussion

For the simulation containing the SCs, it must be pointed out that the voltage significantly decreases because of the behaviour of SCs; when they are discharged the voltage decreases. Next to that, throughout all simulation it can be observed that the current output of the SC or battery is lower when installed at the GS. This is because the transmission line acts as additional series impedance that limits the current.

When comparing the two simulations with varied resistance (i.e. Fig. 8 and 9b) to each other, it stands out that the maximum current supplied by the battery is lower for the higher resistance. This means that a higher series resistance limits the current output.

With an increased inductance, the final value of the current supplied by the battery is the same, however, it takes more time to reach this value. This means, that a higher series inductance increases the response time, which is bad for this research. This longer response time also affects the voltage, which has a longer settling period.

Generally speaking for all the values the following can be said: the larger the value of the resistance and inductance, the smaller and slower the response to the event is, respectively.

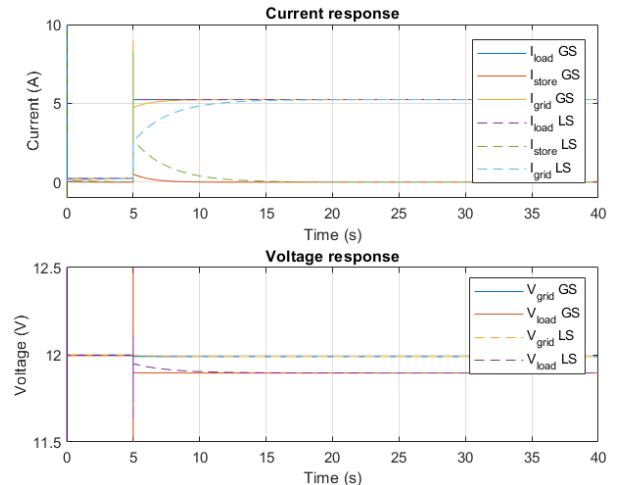


Fig. 5: Results of the simulations with the SC. The solid lines represent the results with the SC installed at the GS, the dashed lines represent the results with the SC installed at the LS.

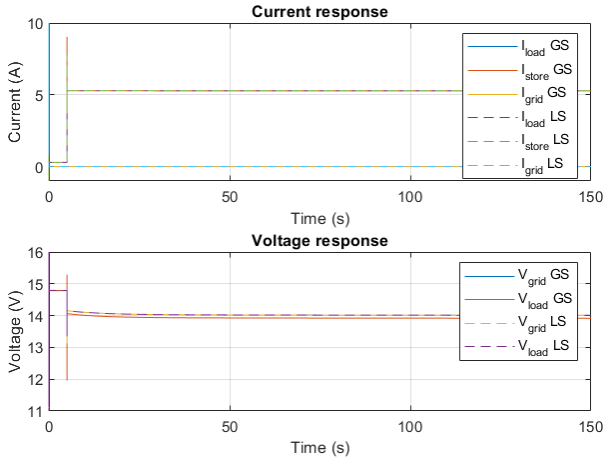


Fig. 6: Results of the simulations with the battery having 80% SoC. The solid lines represent the results with the battery installed at the GS, the dashed lines represent the results with the battery installed at the LS.

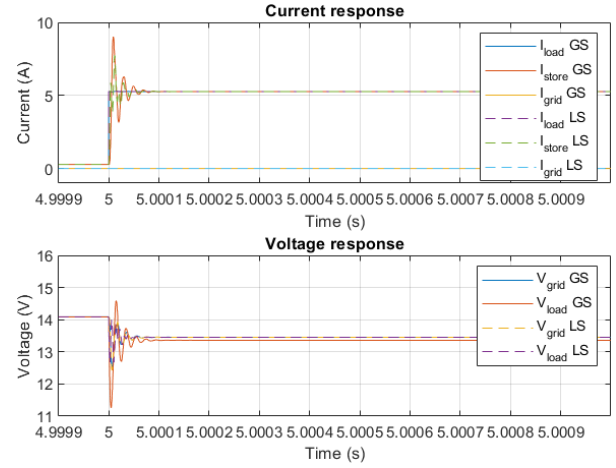


Fig. 8: Results of the simulations with the battery having 10% SoC with a scaled x axis compared to Fig. 7. The solid lines represent the results with the battery installed at the GS, the dashed lines represent the results with the battery installed at the LS.

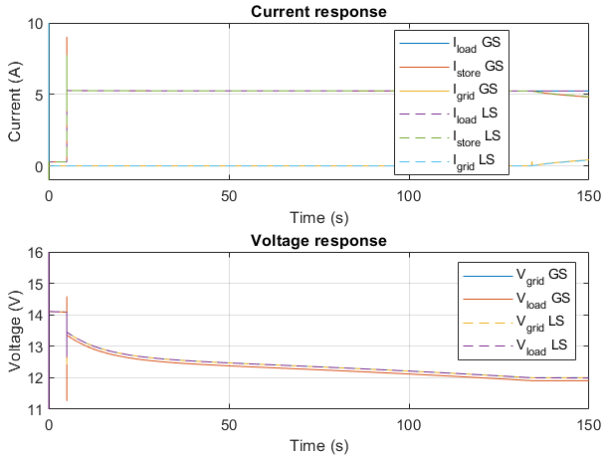


Fig. 7: Results of the simulations with the battery having 10% SoC. The solid lines represent the results with the battery installed at the GS, the dashed lines represent the results with the battery installed at the LS.

The SoC of the battery determines how long the battery is able to cover the inrush current event. Once the battery is drained the current supplied by the grid supply slowly increases, as can be seen in Fig. 7. However, this advantage only holds when the series resistance or inductance of the battery is sufficiently low. If this is not the case the initial peak current that the grid supply needs to deliver is higher compared to the simulation with the SCs.

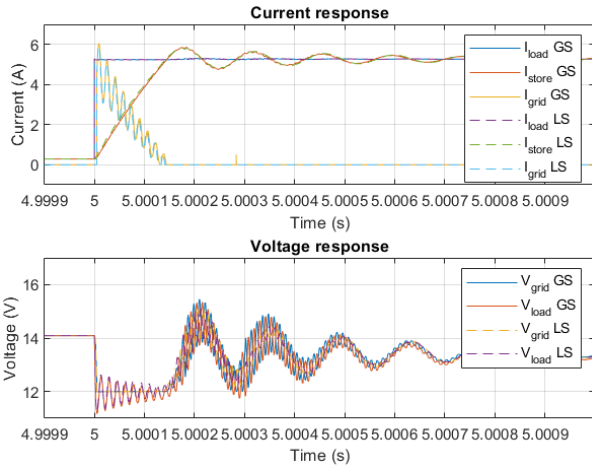
V. EXPERIMENT

A. Experimental setup

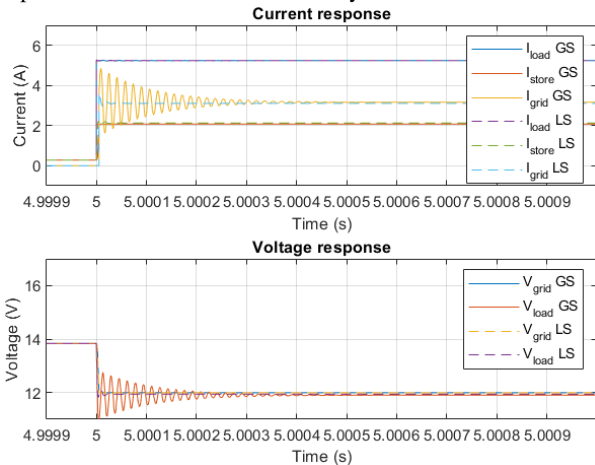
For this experiment the following equipment and components were used:

- Supply: The Rohde & Schwarz HMP2030 Programmable Power Supply is used, because it meets the demands for this experiment and is available in the lab.

- Load: The BK Precision 8601 DC Electronic Load is used, because it meets the demands for this experiment and is available in the lab.
- Data acquisition device: The Picoscope 4824A 8 channel oscilloscope and its accompanying software PicoScope 7 T&M are used to save the data of the three current sensors and the two voltage probes during the experiment.
- Current sensors: The ACS712 Hall Effect-based linear current sensors with a rating of 20 A are used. The sensor output is a voltage that is dependent on the current. For 0 A this is half the supply voltage. It was chosen to not use the 5 A sensor because it would be operating close to its boundary. This is not desirable since it limits the precision of the sensor at the boundaries.
- SC: The SCs used are the WCAP-SISC SCs (EDLCs) from WürthElektronik with a capacity of 350 F per SC. To get the desired voltage level, 5 SCs are connected in series. These particular SCs were chosen because of their availability in the lab and their current rating would not create any bottlenecks in this experiment.
- Battery: The Li-ion battery cells used are LG INR18650MJ1 with a capacity of 3500 mA h and a nominal voltage of 3.7 V each. To get the voltage level that is desired, four 18650 cells are connected in series. These particular cells were chosen because of their availability in the lab and their current rating would not create any bottlenecks in this experiment.
- Battery management system (BMS): The BMS 4S 30A protection circuit with balancing functionality from Otronic.nl was used to secure the safe operation with the Li-ion battery. This is the battery connection to the circuit.
- Cable: A 2 m speaker cable with a diameter of 4 mm was used. This diameter is very much capable of carrying 5 A without significantly heating up. A heated cable is not desirable since the resistance of the cable increases with rising temperature. This would make the measurement



(a) Results of the simulations with the battery having 10% SoC and a series inductance of $50 \mu\text{H}$. The solid lines represent the results with the battery installed at the GS, the dashed lines represent the results with the battery installed at the LS.



(b) Results of the simulations with the battery having 10% SoC and a series resistance of 1Ω . The solid lines represent the results with the battery installed at the GS, the dashed lines represent the results with the battery installed at the LS.

Fig. 9: Graphical representation scaled to the point of impact with the varied series resistance and series inductance

unreliable and not repeatable, and increase the transmission losses. This is not an issue for the scaled model but gets important for the real world application.

Before starting the experiment with the SCs, it was checked whether the SCs are in balance (i.e. having the same voltage across every SC) and stay so during discharge. This can be an issue if the unbalance is so high that some SCs would exceed their rating. When charging the pack to 12 V, none of the SCs exceeded their rating. However, there was one SC that had a slightly lower voltage. By slowly discharging (i.e. using a current of 500 mA), it was found that discharging to a voltage of 3 V for the complete pack still includes a sufficiently high safety margin to avoid discharging to a negative voltage, which would be exceeding the rating.

To be able to have a higher accuracy in the experiment, reference measurements were performed with all three current

sensors. This was done in the expected range of -5 to 5 A in steps of 1 A. Afterwards, this data was evaluated using Matlab. Per current sensor and current value the average voltage has been obtained. Using the `polyfit` function the approximated best fit was computed for each sensor, from which the conversion formula was derived. For completeness, all data and Matlab code can be found in the appendix on page 9.

B. Results

In Fig. 10a, the response to a 5 A inrush current event with SCs installed at the load side can be seen. The response to this event with SCs installed at the GS can be seen in Fig. 10c. The difference in GS and LS installation that was already seen in the simulation results can also be seen here: the SCs are discharged quicker when they are installed at the GS. Next to that, the voltage at the LS is lower when the SCs are installed at the GS compared to when they are installed at the LS. The voltage at the GS is the same as soon as the system is in steady state again, however the initial drop at the 5 A event is slightly higher when the SCs are installed at the GS.

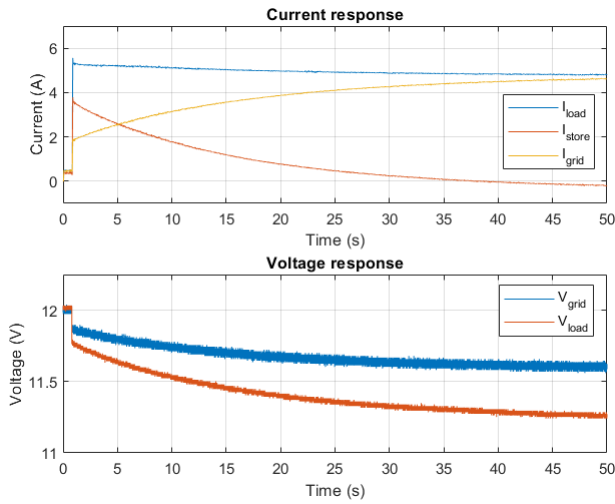
Fig. 10b shows the response to the inrush current event with the battery installed at the LS and Fig. 10d shows the same with the battery installed at the GS. At the moment the inrush current event starts, both the grid supply and the battery start supplying current. When the battery is installed at the LS, the initial peak in the grid supply current is higher compared to when the battery is installed at the GS. In the latter case the voltage at the LS is lower and the peak voltage drop is much higher than when the battery is installed at the LS. The voltage at the supply is in both cases the same.

C. Discussion

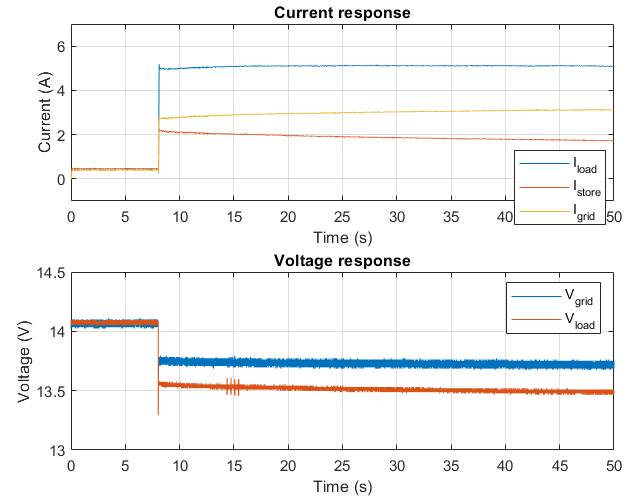
When comparing the experimental results of the SC and the battery it can be seen that the voltage at the start (i.e. without current load) is 12 V with the SC and more than 14 V with the battery. This higher voltage with the battery comes from the battery voltage, that is 14.8 V for a fully charged battery pack. For the experiment with the battery it was chosen to increase the grid supply voltage to 14 V to be able to drain the battery without damaging the cells. This would not be possible with 12 V because the cells would exceed the minimum ratings stated in the datasheet [13]. Although this reduces the comparability between the two experiments, the key outcomes are still clear.

In the graphs some oscillations are visible. To be precise: in Fig. 10c in the current graph from 20 to 25 s, in Fig. 10b in the load voltage at 15 s and in Fig. 10d in the load voltage at 40 s. These oscillations are external interference from other measurements performed simultaneously in the same lab and can safely be ignored.

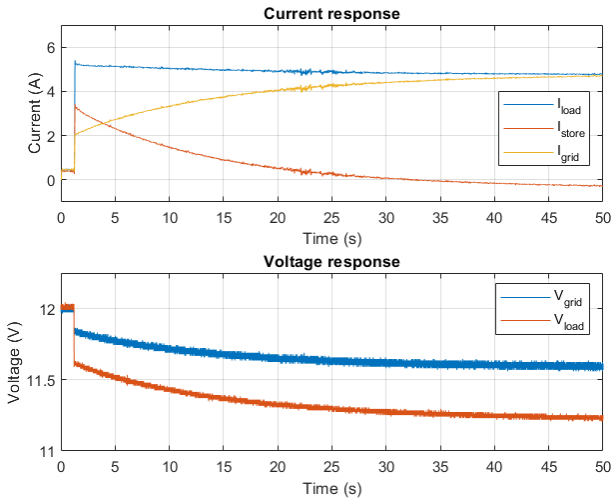
The data of the current sensors contain a lot of noise. Although it can be removed almost completely using a digital filter in Matlab, it is still interesting where that noise comes from. When obtaining the frequency information of the data, it can be seen that the frequency of the noise is not 50 Hz, and that the frequency changes with a change in sampling frequency. To check whether the noise comes from within the



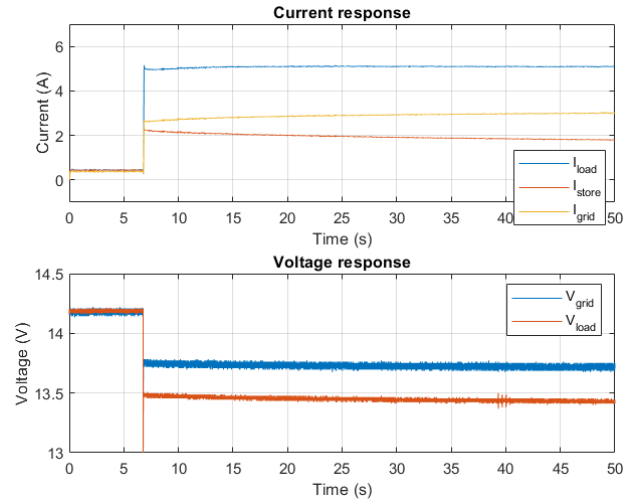
(a) Response to a 5 A inrush current event with SCs installed at the LS



(b) Response to a 5 A inrush current event with a Li-ion battery installed at the LS



(c) Response to a 5 A inrush current event with SCs installed at the GS



(d) Response to a 5 A inrush current event with a Li-ion battery installed at the GS

Fig. 10: Graphical representation of the experimental results

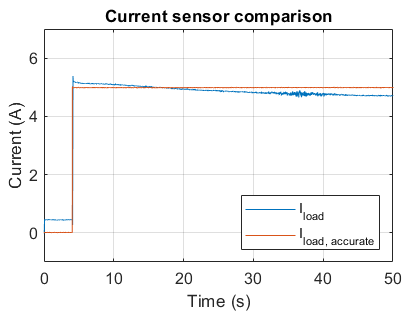


Fig. 11: Comparison of the current sensor used in the experiment to another hall-based current sensor from Keysight (N2783B probe and N2779A power supply)

circuit or has an external source, a higher quality current load sensor from Keysight (N2783B probe and N2779A power supply) was connected in such a way that it also measures I_{load} . The results from this measurement can be seen in Fig. 11. The

blue line represents the filtered data obtained with the ACS712 current sensor, the orange line represents the unfiltered data obtained with the Keysight current sensor. As can be seen, the orange line is completely noise-free and thus the noise has its source outside the circuit.

Another thing that can be observed is that the current is dropping in the SC measurement data. This is also because of the sensor that is used, since the high accuracy sensor does not show this behaviour. Most likely the hall sensor stores the magnetic field. This is prevented by a demagnetizer in the Keysight current sensor.

Although this reduces the accuracy of the results that are presented, qualitatively the results are still valid.

Something else to keep in mind is the charging time of the batteries. Although the batteries have the advantage that they keep the voltage high during discharging for a very long time, especially when compared to the behaviour of SCs, the charging time is very long. This means that the grid loses robustness during the time the batteries are charging and thus

they are not able to cover inrush current events. The charging time is a lot less for SCs which keeps the robustness high. Another problem with the batteries, especially when they are connected the same way as in this research, is the need of a higher charging voltage. This charging voltage cannot be provided by the grid. This means an extra converter would be needed to provide a sufficiently high charging voltage.

VI. DISCUSSION

First, with the SCs a similar behaviour can be observed in both the simulation and the experiment, e.g. that the SCs are discharged faster when installed at the grid side. However, the duration of discharging is much shorter in the simulation and also the voltage drop at the LS is much lower with a steady state voltage of 11.9 V (simulation) compared to 11.25 V (experiment).

With respect to the voltage at the LS, for the battery the same holds. This is in steady state with 13.45 V in the experiment lower than 13.9 V in the simulation, but also the GS voltage is with 13.75 V in the experiment lower than 14 V in the simulation. Furthermore, the peaks in the voltage at the LS that occur when the inrush current events starts are qualitatively the same, i.e. the peak drops lower for the installation at the GS. What is different between simulation and experiment is the amount of current that the grid needs to supply. While in the experiment the grid needs to supply directly from the moment the inrush current event starts, in the simulation it is completely inactive until the battery starts draining.

A possible reason for the additional voltage drop in the experiment can be a higher resistance or reactance in the components, that is not (or not sufficiently) taken into account in the simulation. The same reason can also be used for the inactive grid supply with the battery, because it already has a slight peak at the moment the inrush current starts with the higher series inductance and is continuously active with the higher series resistance. It makes sense to measure the impedance of the battery with an impedance analyser to be able to improve the accuracy of the model.

VII. CONCLUSION AND RECOMMENDATION

The different storage devices have a different specific power and specific energy. This is based on the different electrical characteristics, like the series impedance and the chemical structure. Especially the series impedance determines how fast the device is able to react on a sudden demand of current. Generally speaking, a lower series impedance is advantageous for a quick response and thus a lower current from the grid supply.

The setup with a low impedance battery or a SC installed came out to give the best response to the event.

The location where this device is installed in the microgrid is also important. Here the installation on the LS generally gave the better result because the impedance of the storage device is much lower compared to the grid supply impedance (which also includes the transmission line in this case). This ratio decreases when the storage device is installed at the GS.

For further research on this topic the recommendation is to adjust the setup such that the noise is reduced to be able to reach a higher accuracy in the measurement by e.g. changing the current sensors. For better comparability within the experimental results, but also with the simulations, it makes sense to include the programmable load in the Matlab script using its interface to be able to always turn on the load at the same time in the measurement.

Moreover, it can be advantageous to build a RLC model for the experiment instead of using an actual cable to be able to use parameters that occur in the real world situation as well as to have a better expectation how this result will extrapolate. Next to that determining the impedance of the battery and SC using an impedance analyser could improve the model parameters and therefore the accuracy of the simulation.

REFERENCES

- [1] United Nations, "SDG 7," 2022. [Online]. Available: <https://sdgs.un.org/goals/goal7>
- [2] United Nations, "The Sustainable Development Goals Report 2022," 2022. [Online]. Available: <https://unstats.un.org/sdgs/report/2022/The-Sustainable-Development-Goals-Report-2022.pdf>
- [3] A. A. Alkahtani, S. T. Alfalahi, A. A. Athamneh, A. Q. Al-Shetwi, M. B. Mansor, M. A. Hannan, and V. G. Agelidis, "Power Quality in Microgrids Including Supraharmonics: Issues, Standards, and Mitigations," *IEEE Access*, vol. 8, pp. 127 104–127 122, 2020, doi: 10.1109/ACCESS.2020.3008042.
- [4] P. Q. Blog, "Revised IEC and IEEE standards for PQ measurements for users of PQ monitoring equipment," July 2021. Accessed: June, 27, 2023. [Online]. Available: <https://powerquality.blog/2021/07/30/revised-iec-and-ieee-standards-for-pq-measurements-for-users-of-pq-monitoring-equipment/>
- [5] E. F. Fuchs and M. A. Masoum, "Introduction to Power Quality", Burlington: Academic Press, 2008 pp. 1–54. Accessed: June, 09, 2023. [Online]. doi: 10.1016/B978-012369536-9.50002-4.
- [6] I. E. Commission, "IEV ref 617-04-22," 2017. Accessed: June, 19, 2023. [Online]. Available: <https://www.electropedia.org/iev/iev.nsf/display?openform&ievref=617-04-22>
- [7] D. E. Olivares, A. Mehrizi-Sani, A. H. Etemadi, C. A. Cañizares, R. Iravani, M. Kazerani, A. H. Hajimiragha, O. Gomis-Bellmunt, M. Saeedifard, R. Palma-Behnke, G. A. Jiménez-Estévez, and N. D. Hatziargyriou, "Trends in Microgrid Control," *IEEE Transactions on Smart Grid*, vol. 5, no. 4, pp. 1905–1919, July 2014, doi: 10.1109/TSG.2013.2295514.
- [8] K. Jithin, G. S. Member, P. P. Haridev, N. Mayadevi, R. H. Kumar, and V. P. Mini, "A Review on Challenges in DC Microgrid Planning and Implementation," *Journal of Modern Power Systems and Clean Energy*, 2022, doi: 10.35833/MPCE.2022.000053
- [9] K. Subasinghage, K. Gunawardane, N. Padmawansa, N. Kularatna, and M. Moradian, "Modern Supercapacitors Technologies and Their Applicability in Mature Electrical Engineering Applications," *Energies* 2022, Vol. 15, Page 7752, vol. 15, no. 20, p. 7752, Oct 2022, doi: 10.3390/en15207752.
- [10] G. J. May, A. Davidson, and B. Monahov, "Lead batteries for utility energy storage: A review," *Journal of Energy Storage*, vol. 15, pp. 145–157, Feb. 2018, doi: 10.1016/j.est.2017.11.008. [Online]. Available: <https://linkinghub.elsevier.com/retrieve/pii/S2352152X17304437>
- [11] S. J. Moura, J. B. Siegel, D. J. Siegel, H. K. Fathy, and A. G. Stefanopoulou, "Education on vehicle electrification: Battery Systems, Fuel Cells, and Hydrogen," *2010 IEEE Vehicle Power and Propulsion Conference*, Lille, France, 2010, pp. 1–6, doi: 10.1109/VPPC.2010.5729150.
- [12] R. Kalbitz, "ANP109 — Impedance Spectra of Different Capacitor Technologies," Aug. 2022. Accessed: June, 27, 2023. [Online]. Available: <https://www.wonline.com/components/media/6720421v410%20ANP109a%20EN.pdf>
- [13] S. K. Oh and D. M. Kim, "Product Specification Rechargeable Lithium Ion Battery, Model: INR18650 MJ1 3500mAh," Aug. 2014. Accessed: June, 19, 2023. [Online]. Available: <https://www.tme.eu/Document/5c2d6c3af4c7f80dd8c049bf502c2666/INR18650-MJ1.pdf>

APPENDIX

REFERENCE MEASUREMENT OF THE CURRENT SENSOR

As already stated earlier, the raw data was averaged per current sensor and current value. These average values can be seen in Table IV.

TABLE IV: Reference measurement values of the current sensors

Current (A)	Voltage sensor 1 (V)	Voltage sensor 2 (V)	Voltage sensor 3 (V)	Zeroed voltage sensor 1 (V)	Zeroed voltage sensor 2 (V)	Zeroed voltage sensor 3 (V)
-5	1.9984	1.9949	1.9991	-0.5037	-0.5105	-0.5071
-4	2.0914	2.091	2.0946	-0.4107	-0.4144	-0.4116
-3	2.1873	2.1908	2.1937	-0.3148	-0.3146	-0.3125
-2	2.2901	2.2923	2.295	-0.212	-0.2131	-0.2112
-1	2.3911	2.3967	2.3977	-0.111	-0.1087	-0.1085
0	2.5021	2.5054	2.5062	0	0	0
1	2.5788	2.5818	2.5814	0.0767	0.0764	0.0752
2	2.6562	2.6578	2.6562	0.1541	0.1524	0.15
3	2.7319	2.7324	2.7298	0.2298	0.227	0.2236
4	2.8083	2.8075	2.8027	0.3062	0.3021	0.2965
5	2.8837	2.8828	2.8756	0.3816	0.3774	0.3694

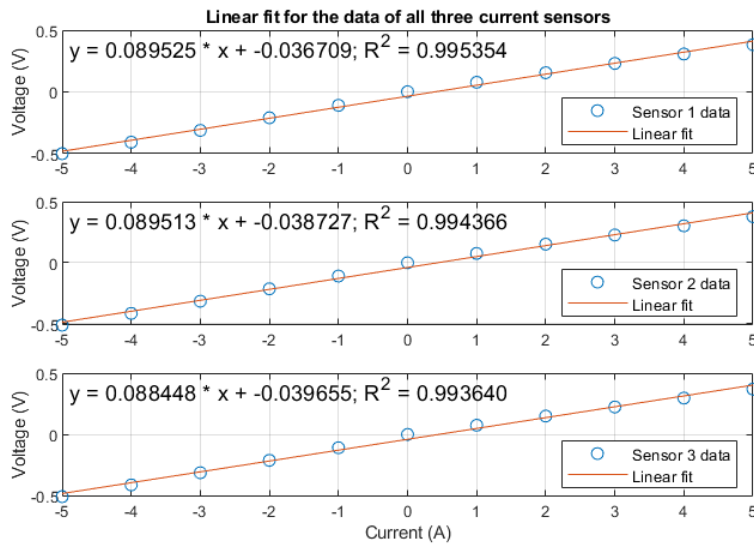


Fig. 12: Linear fit graphs for the data of all current sensors. The x axis contains the current values in the range between -5 to 5 A, the y axis the corresponding zeroed voltage that is at the output of the sensors

This table is imported into Matlab and processed with the `polyfit` function. The linear fit graphs for all three current sensors can be seen in Fig. 12. The resulting equations of the graphs as well as the R^2 values are also visible there.

MATLAB CODE

A. Simulation script

```
1 %% Code to plot simulation results from model_GS.slx
2
3 %close all;
4 clear all;
5
6 simtime = 360;      % Simulation time in s
7 t_inrush = 5;      % Time when inrush current event happens in s
8 I_inrush = -5;     % Value of inrush current in A,
9 % negative means current draw
10
11 % Battery parameters
12 R_bat = 1e-1;      % Battery series resistance
13 L_bat = 5e-7;      % Battery series inductance
14 bat_soc = 80;     % SoC of battery
15
16 % SC parameters
17 C_SC = 350;
18 R_ESR = 3.5e-3;
19 L_ESL = 5e-9;
20 R_leak = 10e6;
21 C_init = 2.4;
22
23
24 simOut_LS = sim('model_GS.slx',simtime);
25 t_LS = simOut_LS.tout;
26
27 I_grid_LS = simOut_LS.simout_LS.signals.values(:,1);
28 I_load_LS = simOut_LS.simout_LS.signals.values(:,2);
29 I_SC_LS = simOut_LS.simout_LS.signals.values(:,3);
30 I_bat_LS = simOut_LS.simout_LS.signals.values(:,4);
31 V_grid_LS = simOut_LS.simout_LS.signals.values(:,5);
32 V_load_LS = simOut_LS.simout_LS.signals.values(:,6);
33 V_bat_LS = simOut_LS.simout_LS.signals.values(:,7);
34 I_store_LS = simOut_LS.simout_LS.signals.values(:,8);
35 V_SC_LS = simOut_LS.simout_LS.signals.values(:,9);
36
37 %%
38 simOut_GS = sim('model_GS.slx',simtime);
39 %%
40 t_GS = simOut_GS.tout;
41
42 I_grid_GS = simOut_GS.simout_GS.signals.values(:,1);
43 I_load_GS = simOut_GS.simout_GS.signals.values(:,2);
44 I_SC_GS = simOut_GS.simout_GS.signals.values(:,3);
45 I_bat_GS = simOut_GS.simout_GS.signals.values(:,4);
46 V_grid_GS = simOut_GS.simout_GS.signals.values(:,5);
47 V_load_GS = simOut_GS.simout_GS.signals.values(:,6);
48 V_bat_GS = simOut_GS.simout_GS.signals.values(:,7);
49 I_store_GS = simOut_GS.simout_GS.signals.values(:,8);
50 V_SC_GS = simOut_GS.simout_GS.signals.values(:,9);
51
52 %% Plot figures
53 subplot(2,1,1)
54 plot(t_GS,I_load_GS, 'DisplayName', 'I_{load} GS', 'Color', [0 0.4470 0.7410], 'LineStyle','-')
55 hold on
56 plot(t_GS,I_store_GS, 'DisplayName', 'I_{store} GS', 'Color', [0.8500 0.3250 0.0980], 'LineStyle','-')
57 hold on
58 plot(t_GS,I_grid_GS, 'DisplayName', 'I_{grid} GS', 'Color', [0.9290 0.6940 0.1250], 'LineStyle','-')
59 hold on
60 plot(t_LS,I_load_LS, 'DisplayName', 'I_{load} LS', 'Color', [0.4940 0.1840 0.5560], 'LineStyle','--')
61 hold on
62 plot(t_LS,I_store_LS, 'DisplayName', 'I_{store} LS', 'Color', [0.4660 0.6740 0.1880], 'LineStyle','--')
63 hold on
64 plot(t_LS,I_grid_LS, 'DisplayName', 'I_{grid} LS', 'Color', [0.3010 0.7450 0.9330], 'LineStyle','--')
65
```

```

66 title('Current response')
67 xlabel('Time (s)')
68 ylabel('Current (A)')
69 legend('Location','east')
70 % xlim([4.9999 5.001])
71 xlim([0 50])
72 ylim([-1 10])
73 grid on
74
75 subplot(2,1,2)
76 plot(t_GS,V_grid_GS, 'DisplayName', 'V_{grid} GS', 'Color', [0 0.4470 0.7410], 'LineStyle','-')
77 hold on
78 plot(t_GS,V_load_GS, 'DisplayName', 'V_{load} GS', 'Color', [0.8500 0.3250 0.0980], 'LineStyle','-')
79 hold on
80 plot(t_LS,V_grid_LS, 'DisplayName', 'V_{grid} LS', 'Color', [0.9290 0.6940 0.1250], 'LineStyle','--')
81 hold on
82 plot(t_LS,V_load_LS, 'DisplayName', 'V_{load} LS', 'Color', [0.4940 0.1840 0.5560], 'LineStyle','--')
83
84
85 title('Voltage response')
86 xlabel('Time (s)')
87 ylabel('Voltage (V)')
88 legend('Location','northeast')
89 % xlim([4.9999 5.001])
90 xlim([0 50])
91 ylim([11 16])
92 grid on

```

B. Current sensor reference measurement

```

1 %% Current sensor reference measurement
2 clc
3 close all
4 clear all
5
6 %% Get data
7 data = readmatrix("Current_sensor_values.csv");
8 % This csv file already contains the preprocessed (i.e. averaged)
9 % measurement data
10 %% Assign data to variables
11 t = data(:,1);
12 sensor_1 = data(:,5);
13 sensor_2 = data(:,6);
14 sensor_3 = data(:,7);
15
16 %% Apply polyfit function to variables
17 [s1_pf, S1] = polyfit(t,sensor_1,1);
18 [s2_pf, S2] = polyfit(t,sensor_2,1);
19 [s3_pf, S3] = polyfit(t,sensor_3,1);
20
21 %% Apply polyval function to be able to plot data
22 s1_pv = polyval(s1_pf,t);
23 s2_pv = polyval(s2_pf,t);
24 s3_pv = polyval(s3_pf,t);
25
26 %% Computing R^2
27 yresid1 = sensor_1 - s1_pv;
28 yresid2 = sensor_2 - s1_pv;
29 yresid3 = sensor_3 - s1_pv;
30
31 SSresid1 = sum(yresid1.^2);
32 SSresid2 = sum(yresid2.^2);
33 SSresid3 = sum(yresid3.^2);
34
35 SStotal1 = (length(s1_pv)-1) * var(sensor_1);
36 SStotal2 = (length(s2_pv)-1) * var(sensor_2);
37 SStotal3 = (length(s3_pv)-1) * var(sensor_3);

```

```

38
39 rsq1 = 1 - SSresid1/SStotal1;
40 rsq2 = 1 - SSresid2/SStotal2;
41 rsq3 = 1 - SSresid3/SStotal3;
42
43 %% Plot data and linear fit for all 3 sensors
44 figure
45 subplot(3,1,1)
46 plot(t,sensor_1,'o',t,s1_pv,'-')
47 title('Linear fit for the data of all three current sensors')
48 xl = xlim;
49 yl = ylim;
50 xt = 0.01 * (xl(2)-xl(1)) + xl(1);
51 yt = 0.87 * (yl(2)-yl(1)) + yl(1);
52 caption = sprintf('y = %f * x + %f; R^2 = %f', s1_pf(1), s1_pf(2), rsq1);
53 text(xt, yt, caption, 'FontSize', 11);
54 grid on
55 legend('Sensor 1 data','Linear fit','location','southeast')
56 ylabel('Voltage (V)')
57 subplot(3,1,2)
58 plot(t,sensor_2,'o',t,s2_pv,'-')
59 xl = xlim;
60 yl = ylim;
61 xt = 0.01 * (xl(2)-xl(1)) + xl(1);
62 yt = 0.87 * (yl(2)-yl(1)) + yl(1);
63 caption = sprintf('y = %f * x + %f; R^2 = %f', s2_pf(1), s2_pf(2), rsq2);
64 text(xt, yt, caption, 'FontSize', 11);
65 grid on
66 legend('Sensor 2 data','Linear fit','location','southeast')
67 ylabel('Voltage (V)')
68 subplot(3,1,3)
69 plot(t,sensor_3,'o',t,s3_pv,'-')
70 xl = xlim;
71 yl = ylim;
72 xt = 0.01 * (xl(2)-xl(1)) + xl(1);
73 yt = 0.87 * (yl(2)-yl(1)) + yl(1);
74 caption = sprintf('y = %f * x + %f; R^2 = %f', s3_pf(1), s3_pf(2), rsq3);
75 text(xt, yt, caption, 'FontSize', 11);
76 grid on
77 legend('Sensor 3 data','Linear fit','location','southeast')
78 xlabel('Current (A)')
79 ylabel('Voltage (V)')

```

C. Plot data from experiments

```

1 %% Create plots from measurement data
2 clc
3 close all
4 clear all
5
6 %% Choose which .csv document is used
7 %data = readmatrix("Data\SC discharge\20230605-0010-Discharge caps 5000mA 2kSs 50s.csv");
8 %data = readmatrix("Data\SC discharge\20230605-0012-Discharge caps 5000mA GS 2kSs 50s.csv");
9 %data = readmatrix("Data\Bat discharge\20230605-0012-Discharge bat 5000mA 2kSs/20230605-0012-Discharge ...
10 bat 5000mA 2kSs_1.csv");
11 %data = readmatrix("Data\Bat discharge\20230605-0006-Discharge bat 5000mA GS ...
12 2kSs/20230605-0006-Discharge bat 5000mA GS 2kSs_1.csv");
13
14 data = readmatrix("Data\Additional current sensor\20230622-0003-SC LS discharge add current sensor.csv");
15
16 t = data(:,1);
17 t = t + abs(t(1,1)); % Remove the offset created by the picoscope to start at t=0
18 V_I_grid = data(:,2);
19 V_I_store = data(:,3);
20 V_I_load = data(:,4);
21 V_grid = data(:,5);
22 V_load = data(:,6);

```

```

21 V_I_load_accurate = data(:,7);
22
23 %% Convert current sensor signal voltage to actual current
24 I_grid = zeros(size(V_I_grid));
25 I_store = zeros(size(V_I_store));
26 I_load = zeros(size(V_I_load));
27 I_load_accurate = 10 * V_I_load_accurate;
28
29 for i = 1:length(V_I_grid)
30 V_I_grid(i) = V_I_grid(i) - 2.5021;
31 I_grid(i) = (V_I_grid(i) + 0.0367) / 0.0895;
32 end
33 for i = 1:length(V_I_store)
34 V_I_store(i) = V_I_store(i) - 2.5054;
35 I_store(i) = (V_I_store(i) + 0.0387) / 0.0895;
36 end
37 for i = 1:length(V_I_load)
38 V_I_load(i) = V_I_load(i) - 2.5034;
39 I_load(i) = (V_I_load(i) + 0.0397) / 0.0884;
40 end
41
42 %% Filter current signals
43 d = firceqrip('minorder',[0.002 0.03],[0.001 0.001]);
44
45 I_grid_filtered = filter(d,1,I_grid);
46 I_store_filtered = filter(d,1,I_store);
47 I_load_filtered = filter(d,1,I_load);
48
49 %% Plot figures
50 figure
51 subplot(2,1,1)
52 plot(t,I_load_filtered, 'DisplayName', 'I_{load}')
53 hold on
54 plot(t,I_store_filtered, 'DisplayName', 'I_{store}')
55 hold on
56 plot(t,I_grid_filtered, 'DisplayName', 'I_{grid}')
57
58 title('Inrush current response')
59 xlabel('Time (s)')
60 ylabel('Current (A)')
61 legend('Location','east')
62 xlim([0 50])
63 ylim([-1 7])
64 grid on
65
66 subplot(2,1,2)
67 plot(t,V_grid, 'DisplayName', 'V_{grid}')
68 hold on
69 plot(t,V_load, 'DisplayName', 'V_{load}')
70
71 title('Voltage at grid and load side')
72 xlabel('Time (s)')
73 ylabel('Voltage (V)')
74 legend()
75 xlim([0 50])
76 %ylim([13 14.5]) % For battery
77 ylim([11 12.5]) % For SC
78 grid on
79
80 figure
81 plot(t,I_load_filtered, 'DisplayName', 'I_{load}')
82 hold on
83 plot(t,I_load_accurate, 'DisplayName', 'I_{load, accurate}')
84
85 title('Current sensor comparison')
86 xlabel('Time (s)')
87 ylabel('Current (A)')
88 legend('Location','southeast')
89 xlim([0 50])

```



```
90 ylim([-1 7])  
91 grid on
```